Multi-sensor Comparison of the NDVI and EVI

Tomoaki Miura

Department of Natural Resources and Environmental Management

University of Hawaii at Manoa, USA

Contributions from:

Javzandulm Tsend-Ayush, University of Hawaii at Manoa, USA
Hiroki Yoshioka, Aichi Prefectural University, Japan
Jesslyn F. Brown, USGS EROS Center, USA
Yingxin Gu, ASRC Technology & Solutions, USGS EROS Center, USA

Introduction – Multi-sensor Vegetation Indices

- A large number of space-borne optical imagers
- Multi-sensor/-platform VI applications
  - Regional mosaics of multi-platform VIs
  - Change detection across multi-sensor VIs
  - Synergistic, multi-resolution VIs
  - Long-term VI records
- Quality of VI products
  - How well each sensor retrieves VIs (e.g., NDVI)
- Compatibility/linkage among VI products
  - How well one sensor's NDVI compares with those from other sensors

Multi-sensor Comparison

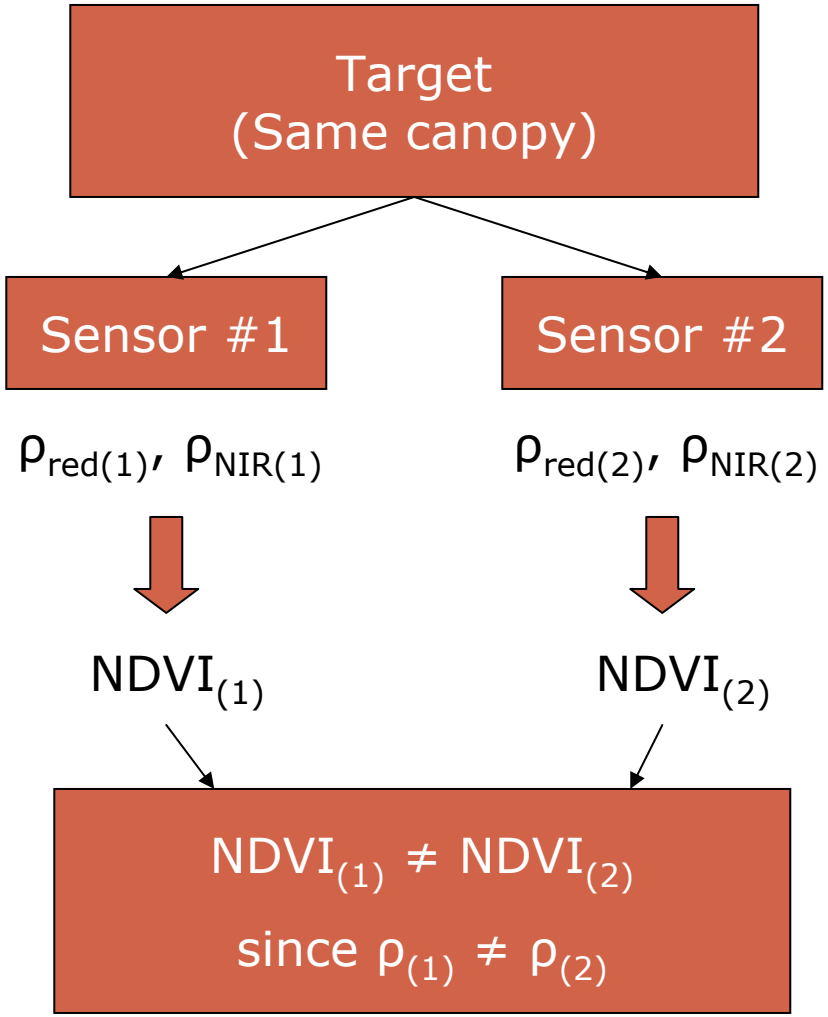

- Sensor/platform characteristics
  - Spectral bandpass
  - Spatial resolution
  - Radiometric resolution
  - Geometric registration
  - Sun-target-view geometry
  - Overpass time
- Algorithms
  - Radiometric calibration
  - Atmospheric correction
  - Temporal compositing
  - Cloud/snow masking

(Yoshioka et al., 2003; Miura et al., 2006; Swinnen & Veroustraete, 2008)

Vegetation Indices – NDVI & EVI

(Huete et al., 2006, White Paper for NASA ESDR/CDR)

- Optical measures of vegetation canopy "greenness" - a direct measure of photosynthetic potential resulting from the *composite* property of total leaf chlorophyll, leaf area, canopy cover, and canopy architecture

- Proxies in estimating canopy state variables (e.g., leaf area index, fractional cover) and canopy biophysical processes (e.g., photosynthesis, net primary production)

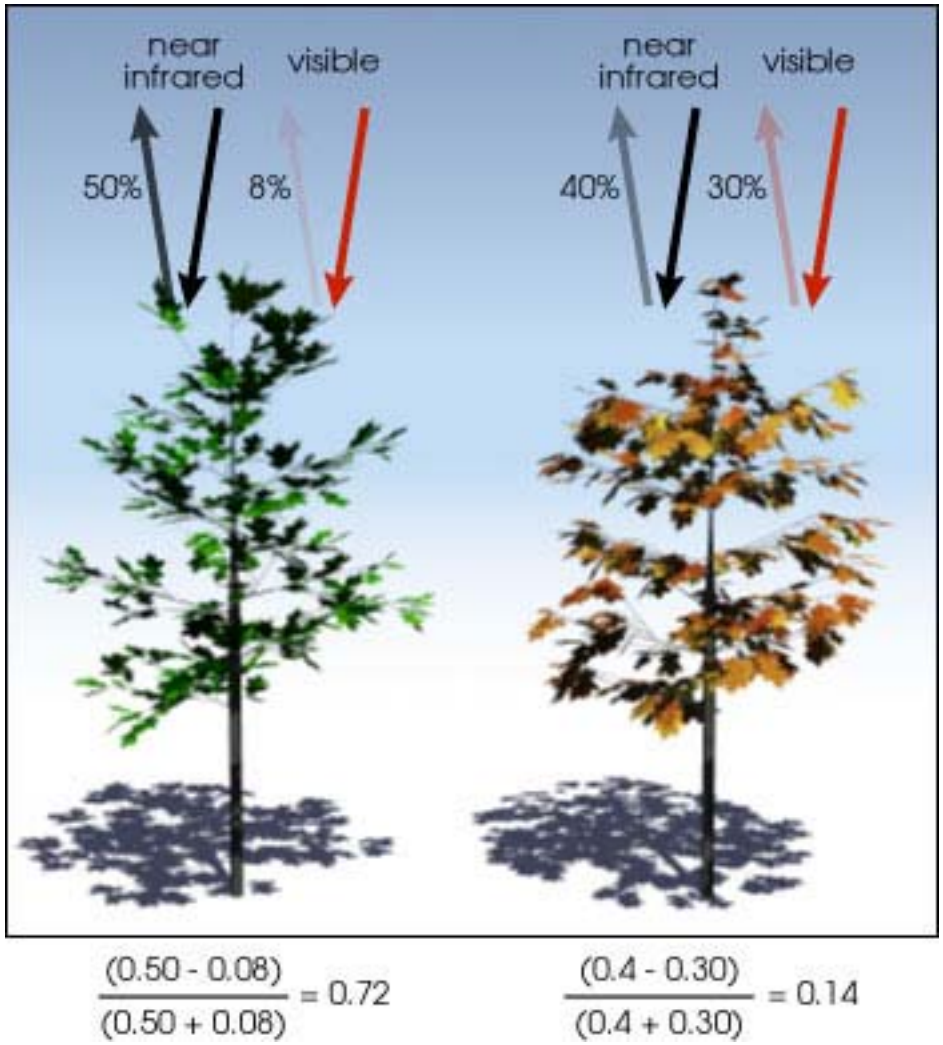

[Source: Earth Observatory – Measuring Vegetation (NDVI & EVI) http://earthobservatory.nasa.gov/Features/MeasuringVegetation/measuring_vegetation_2.php]

Normalized Difference VI

$$NDVI = \frac{\rho_{NIR} - \rho_{red}}{\rho_{NIR} + \rho_{red}}$$

Enhanced VI

$$EVI = G\frac{\rho_{NIR} - \rho_{red}}{\rho_{NIR} + C_1\rho_{red} - C_2\rho_{red} + L}$$

*The adopted coefficients are G=2.5, C1=6, C2=7, and L=1.

Two-band Enhanced VI

$$EVI2 = G'\frac{\rho_{NIR} - \rho_{red}}{\rho_{NIR} + C'\rho_{red} + L'}$$

*The adopted coefficients are G'=2.5, C'=2.4, and L'=1.

(Rouse et al., 1973; Huete et al., 2002; Jiang et al., 2008)

Vegetation Index Cross-comparison Methodologies

1. Top-Down Approach

- Product inter-comparison
- Agreement analysis

2. Bottom-Up Approach

- Modeling/simulation (theoretical/empirical)
- Single factor analysis
- Multiple factor analysis

Sensor Characteristic Differences

ASTER

- VNIR Pushbroom
- VNIR 15m
- ρ_{green}, ρ_{red}, ρ_{NIR}

MODIS

- Whiskbroom
- Land Bands 250m, 500m
- ρ_{blue}, ρ_{green}, ρ_{red}, ρ_{NIR}

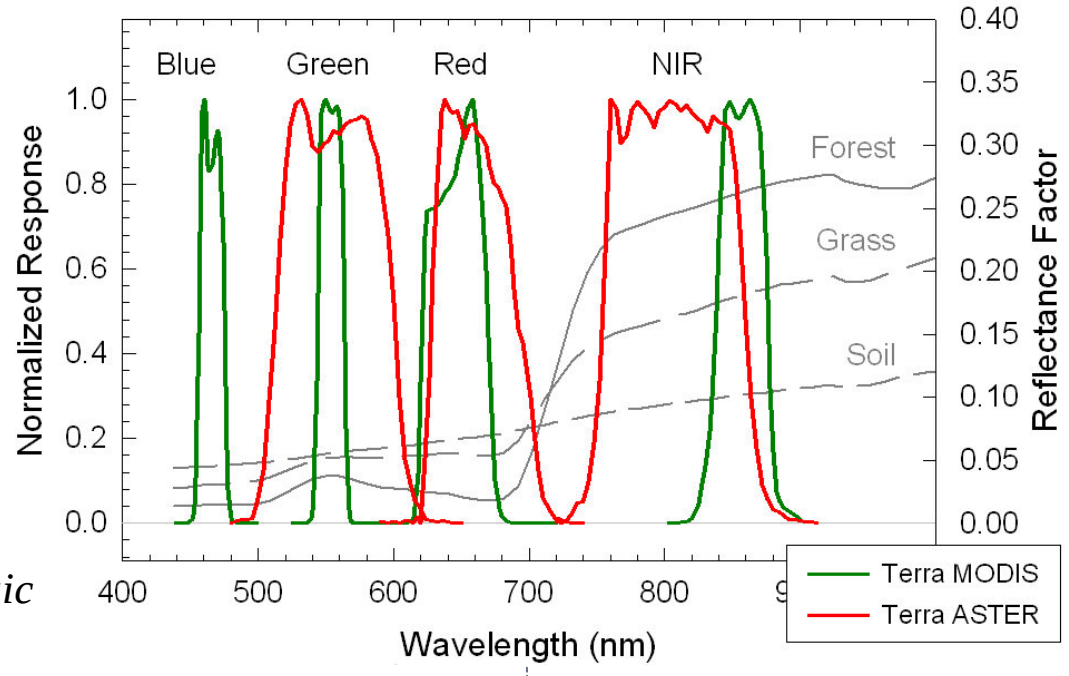

** Not designed to retrieve atmospheric information*

Spectral Bandpass Differences: *EO-1 Hyperion*

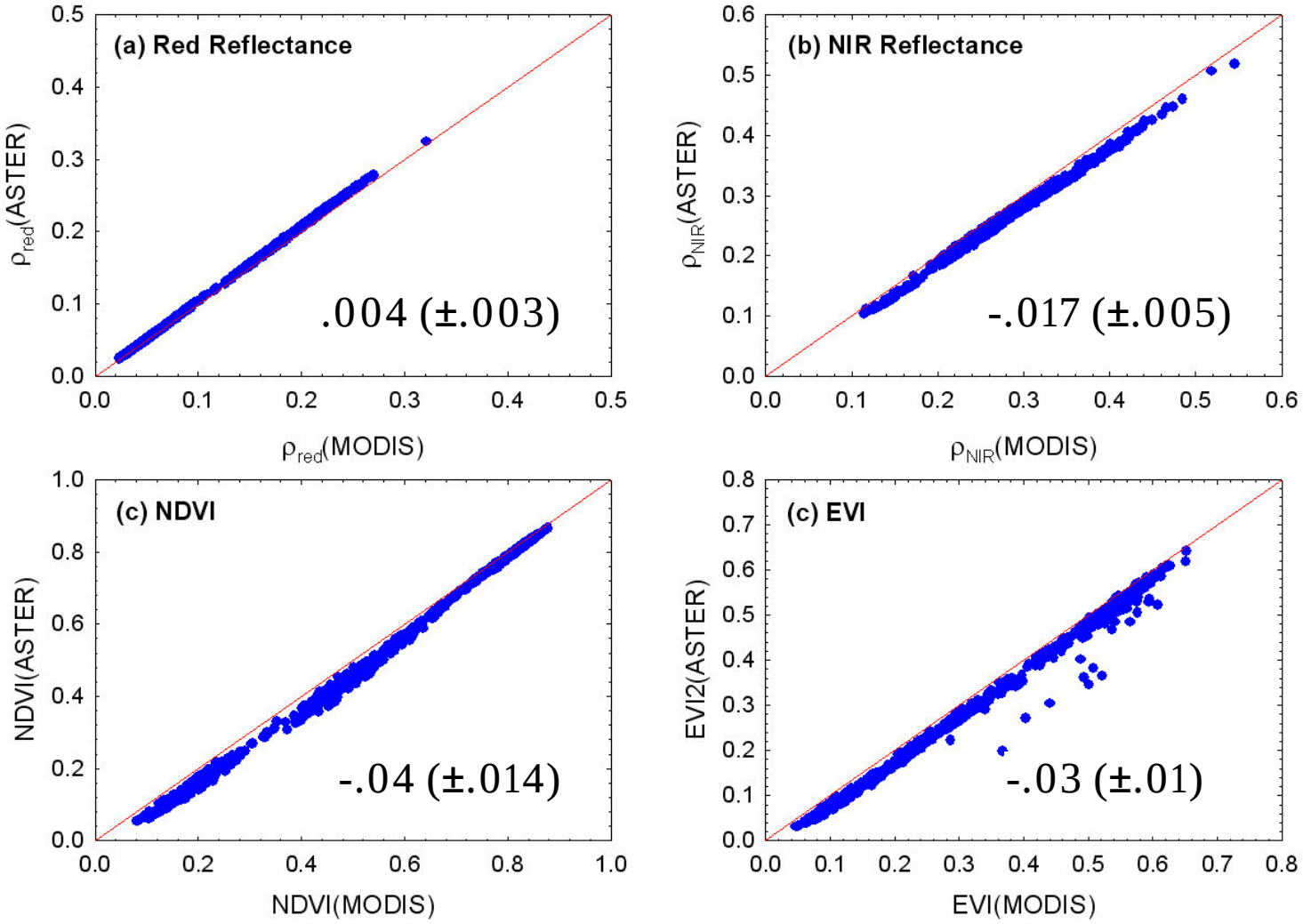

ASTER vs. MODIS Algorithm Differences

	ASTER	MODIS
PGE Version	3.1	4.0.10
TOA Irradiance	WRC exo-atmospheric solar irradiance (absolute calibration accuracy: 4%)	None – Direct computation of TOA reflectance by ratioing to the solar diffuser (calibration accuracy: 2%)
Approach	Combined LUT-matching and on-time MODTRAN computation (Thome et al., 1998): • LUT generated by a Gauss-Seidel iteration code • Scattering terms by LUT-matching & gaseous transmission terms by MODTRAN	Combined LUT-interpolation and on-time 6S computation (Vermote et al., 2006): • LUT generated by the 6S code • Molecular terms by on-time 6S computation & aerosol terms by LUT-interpolation
Pressure	NCEP GDAS adjusted for local elevation using GTOPO30	NCEP GDAS adjusted for local elevation using GTOPO30
Ozone	NCEP TOVS	NASA TOMS
Water Vapor	NCEP GDAS	MODIS water vapor
Aerosol	No correction	MODIS aerosols
Theoretical Accuracy	14% for $\rho < 0.1$ 7% for $\rho > 0.1$	5% for clear aerosol loading 9% for high aerosol loading

(Miura et al., 2008)

Global Comparison:
ASTER (AST07XT) vs. MODIS (MOD09GHK)

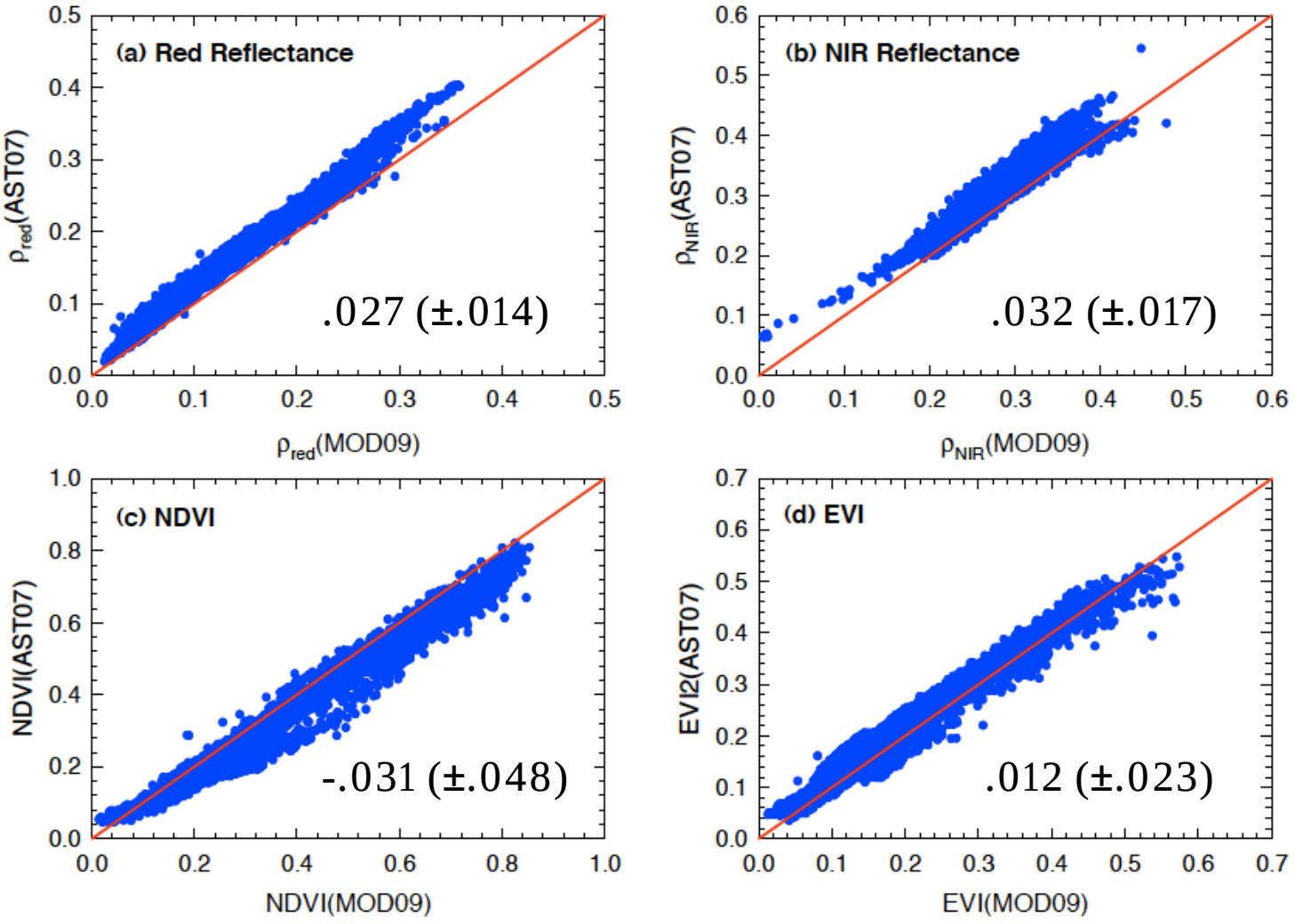

(Miura et al., 2008)

Multi-site Comparison:
ASTER (Aeronet) vs. MODIS (Aeronet)

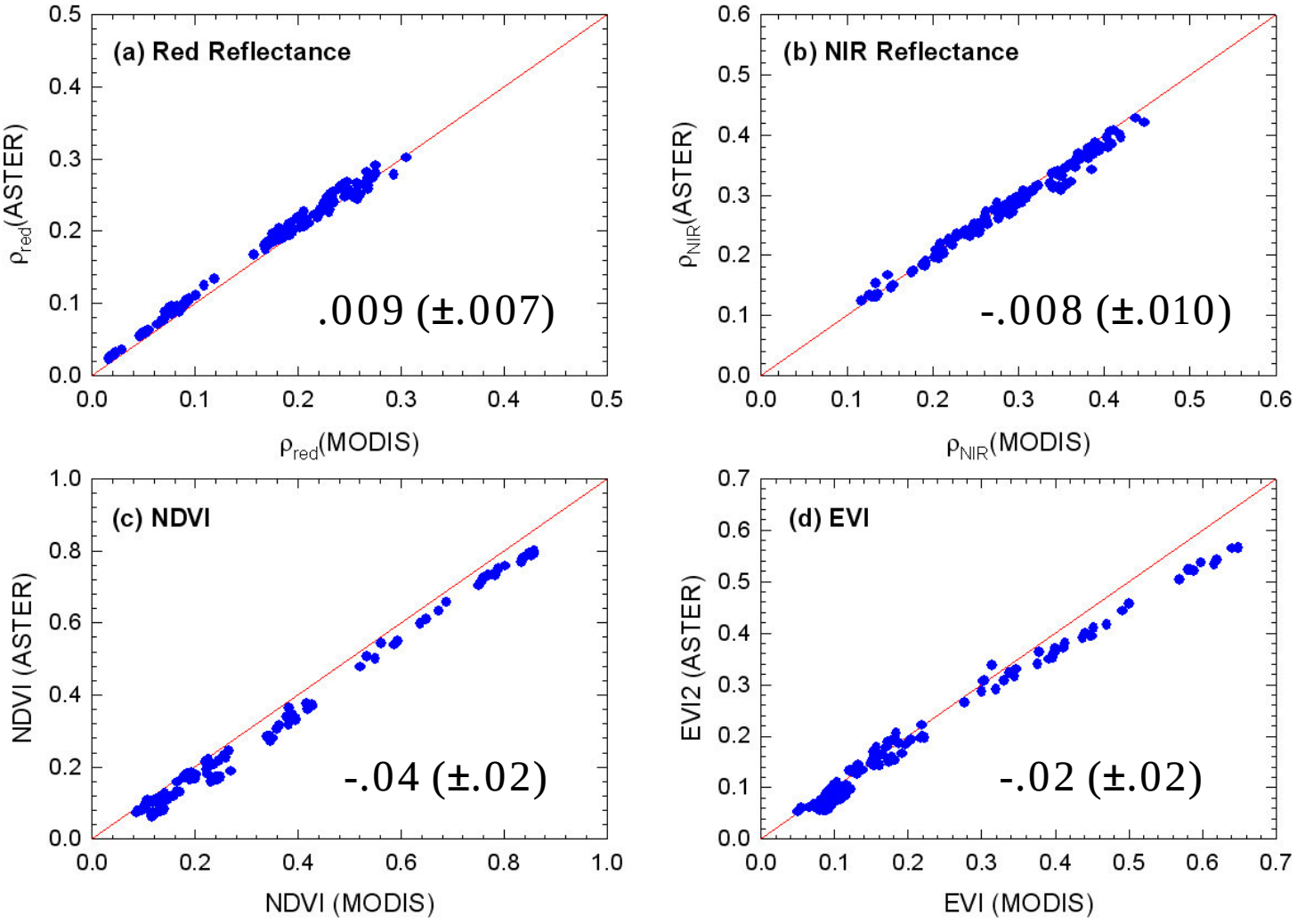

(Miura et al., 2008)

Cross-sensor/-platform Comparison over CONUS: MODIS, AVHRR/2, AVHRR/3, vs. VEGETATION

	Terra MODIS	Aqua MODIS	NOAA-14 AVHRR/2	NOAA-17 AVHRR/3	SPOT-4 VEGETATION
Altitude	705 km		850 km		830 km
Orbit	Near-polar, sun-synchronous		Near-polar, sun-synchronous		Near-polar, sun-synchronous
Inclination	98.2°		99°		98.7°
Orbit period	99 minutes		102 minutes		101 minutes
Repeat cycle	16 days		9 days		26 days
Equator crossing time	10:30 am (descending)	1:30 pm (ascending)	1:30 pm - 5:00 pm (ascending)	10:00 am (descending)	10:30 am (descending)
Swath width	110° (±55°), 2,330 km (whiskbroom)		110° (±55°), 2,800 km (whiskbroom)		101°, 2,250 km (pushbroom)
Spatial resolution	<u>Band 1 and 2</u> 250 m at nadir 0.4-by-0.7 km at $\theta_v = 55°$ 0.5-by-1.2 km at edge ($\theta_v = 65.4°$) <u>Band 3 - 7</u> 500 m at nadir 0.8-by-1.4 km at $\theta_v = 55°$ 1-by-2.4 km at edge ($\theta_v = 65.4°$)		1.1 km at nadir 1.7-by-3 km at $\theta_v = 55°$ 2-by-6 km at edge ($\theta_v = 68°$)		1.15 km at nadir 1.15-by-2.2 km at $\theta_v = 55°$ 1.15-by-2.5 km at edge ($\theta_v = 60°$)

Cross-sensor/-platform Comparison over CONUS (1 km): MODIS, AVHRR/2, AVHRR/3, vs. VEGETATION

	Terra MODIS	Aqua MODIS	NOAA-14 AVHRR/2	NOAA-17 AVHRR/3	SPOT-4 VEGETATION
Geolocation accuracy	50 m (RMSE) at nadir		1,000 m (RMSE)		330 m (RMSE)
Resampling method	Nearest neighbor		Nearest neighbor		Cubic convolution
Radiometric calibration	2 %		5 %	5 %	5 %

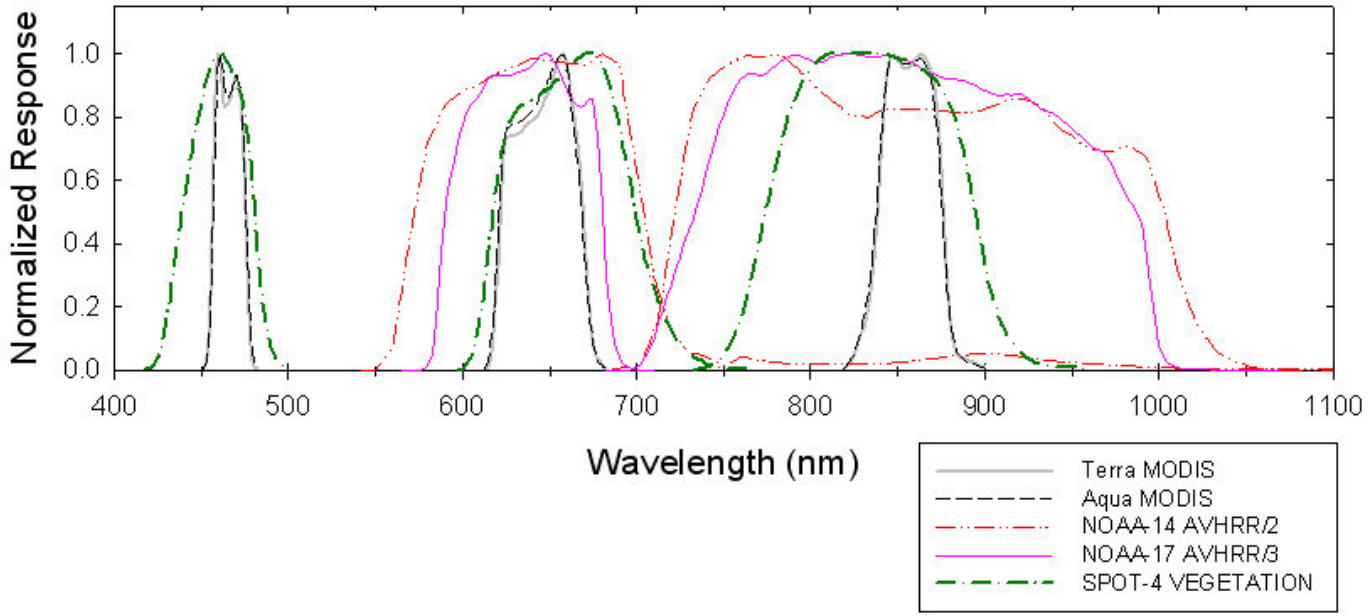

Cross-sensor/-platform Comparison over CONUS:
Satellite Data Products

- Terra & Aqua MODIS (USGS eMODIS)
  - 1 km weekly, CV-MVC
  - corrected for total atmosphere
- SPOT-4 VEGETATION (VITO S10)
  - 1 km weekly (re-composited from 10-day), MVC
  - corrected for total atmosphere
- NOAA-17 AVHRR/3 (USGS EROS)
  - 1 km weekly, MVC
  - corrected for molecular scattering, and ozone and water vapor absorptions
- NOAA-14 AVHRR/2 (USGS EROS)
  - 1 km weekly, MVC
  - corrected for molecular scattering, and ozone and water vapor absorptions

(Source: http://phenology.cr.usgs.gov/index.php)

Footprint Simulation

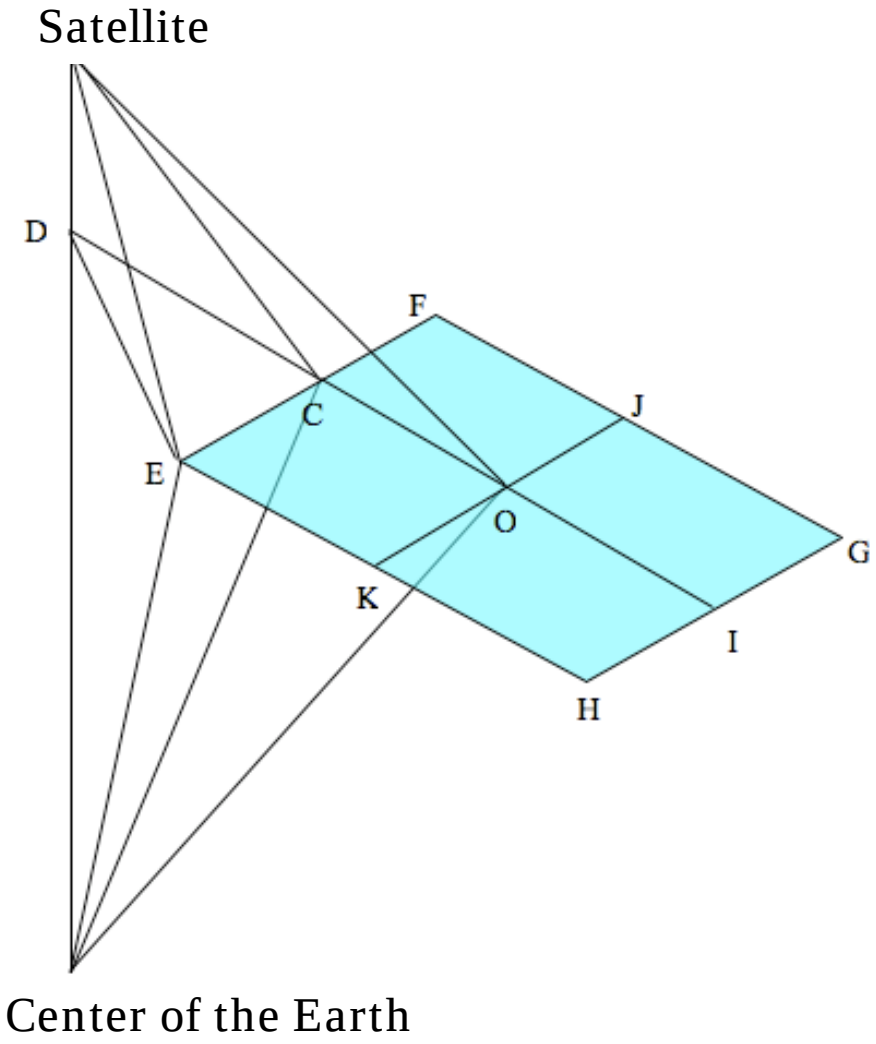

- Changes in footprint size and PSF modeled using a satellite orbital model (Tan et al., 2006)
- Daily basis over a 16-day period in June 2002
  - Terra MODIS
    - 250m/500m at nadir
  - NOAA-16 AVHRR
    - 1.1 km at nadir
  - SPOT-4 VEGETATION
    - 1.1 km at nadir

SPOT-Vegetation
Off Nadir vs Nadir

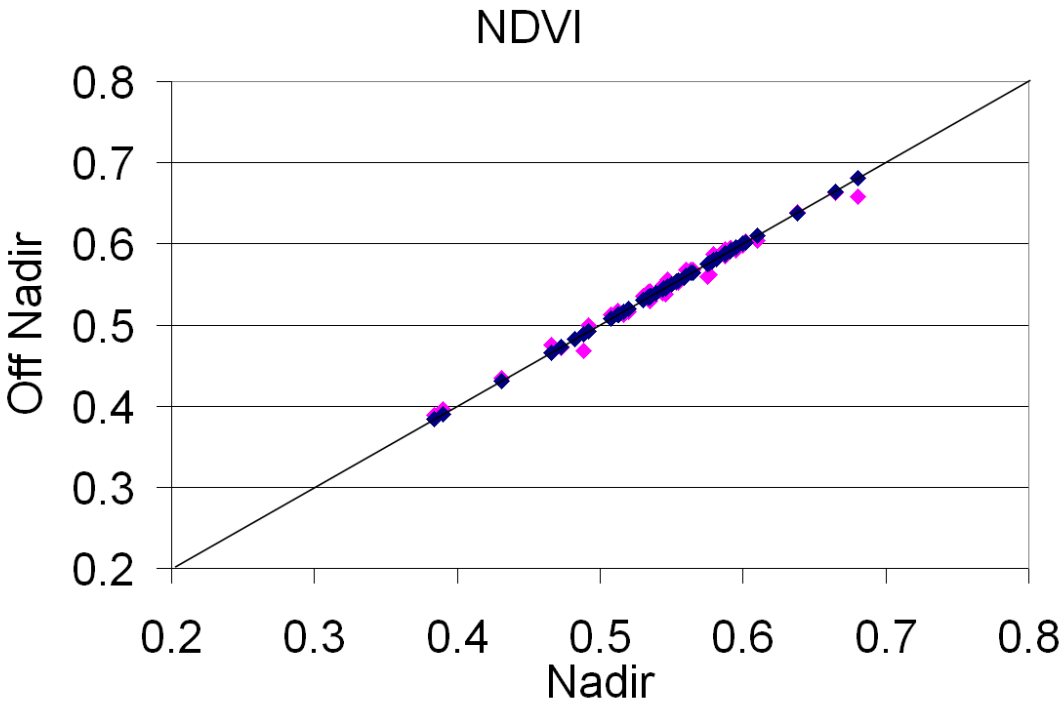

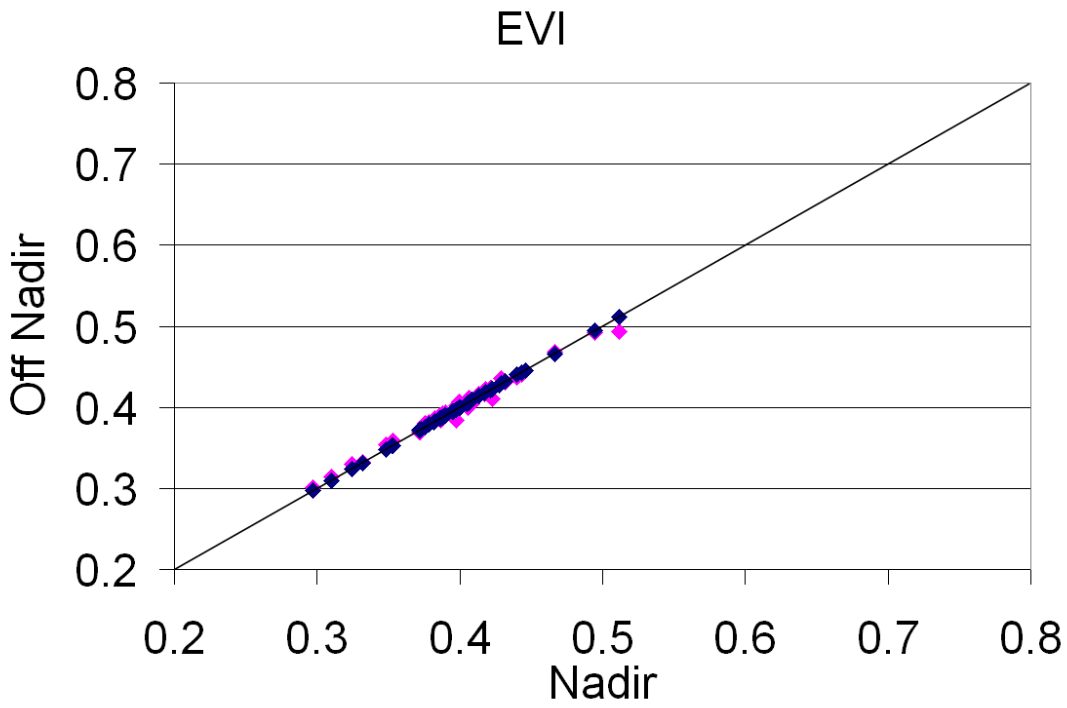

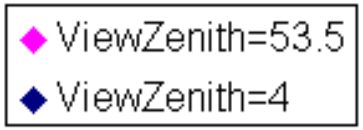

(Miura et al., 2010, in prep.)

SPOT-Vegetation
Off Nadir vs Nadir

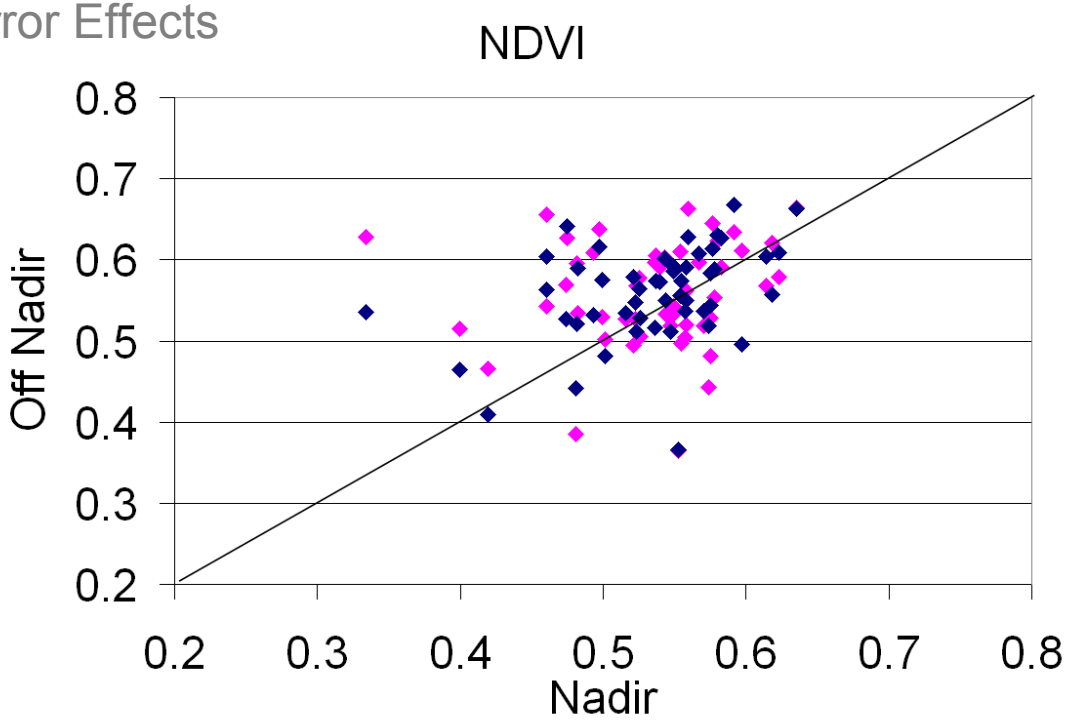

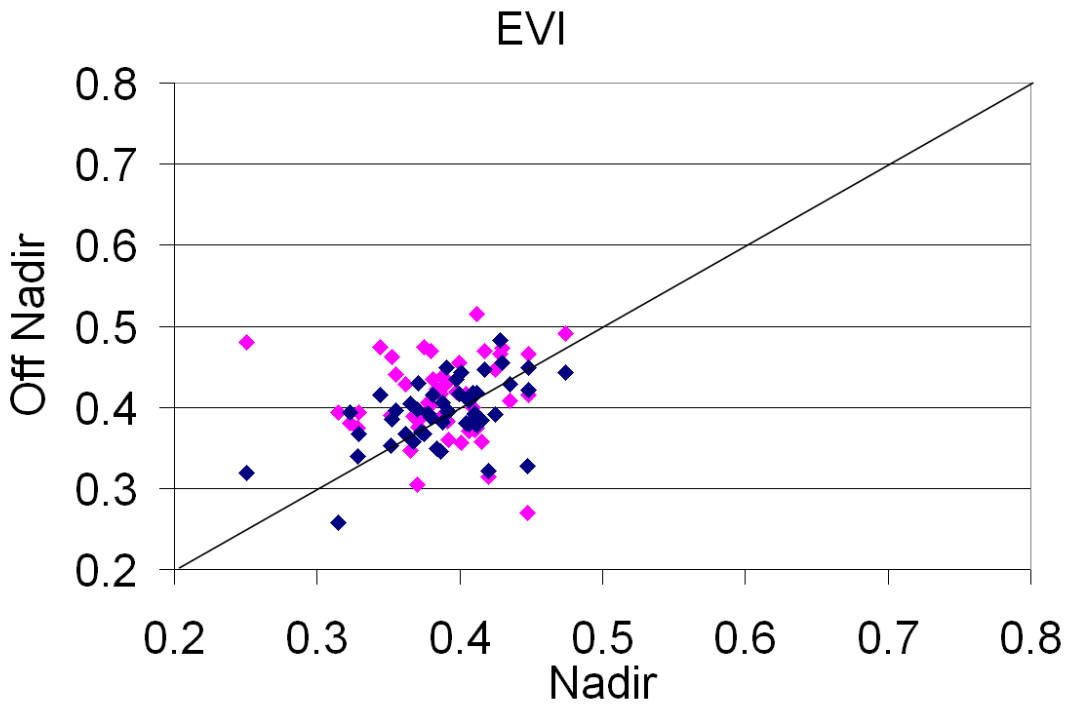

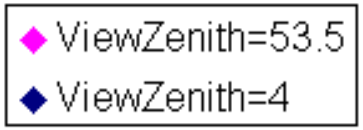

Geolocation Error (m)

X=-480, Y=-1320 (Angle=53.5)

X=-780, Y=-210 (Angle=4)

(Miura et al., 2010, in prep.)

Sensor Comparison ~ NDVI

DOY=175

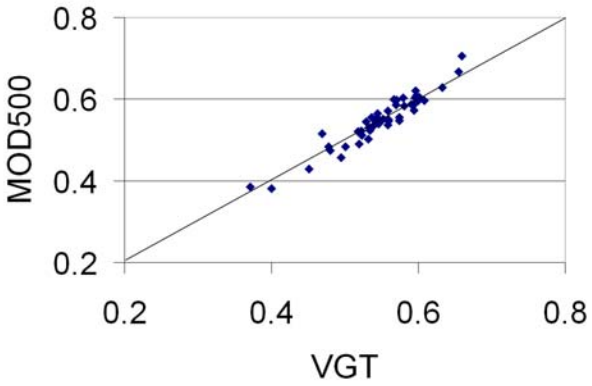

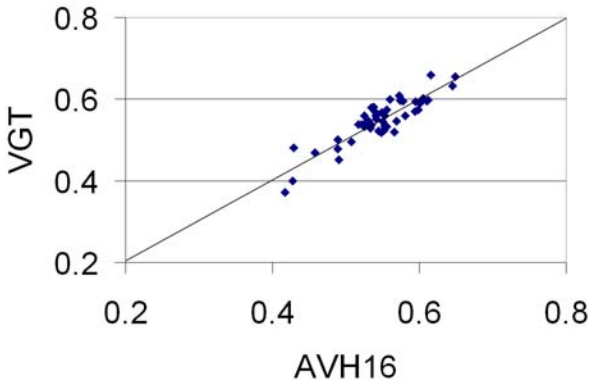

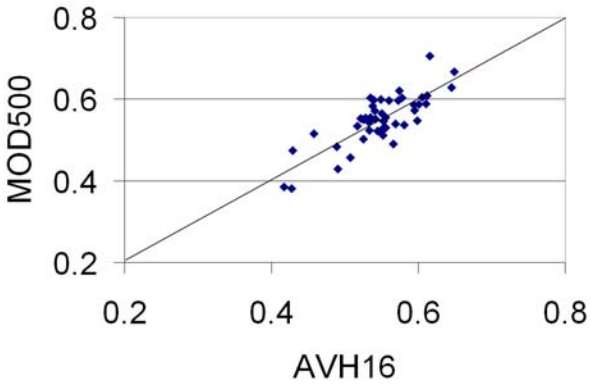

MOD500 = 26º(X=-2, Y=0), AVH16 = 43º (X=0, Y=-8), VGT = 50º (X=1, Y=-6)

DOY=181

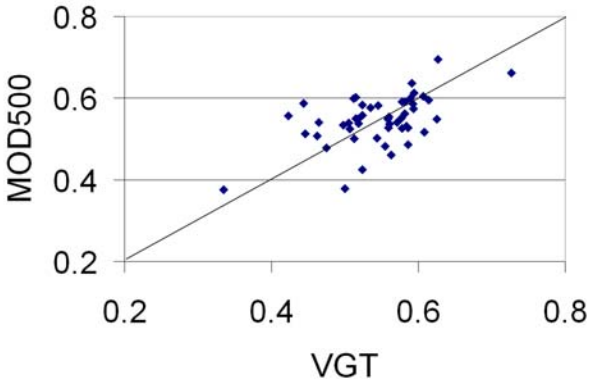

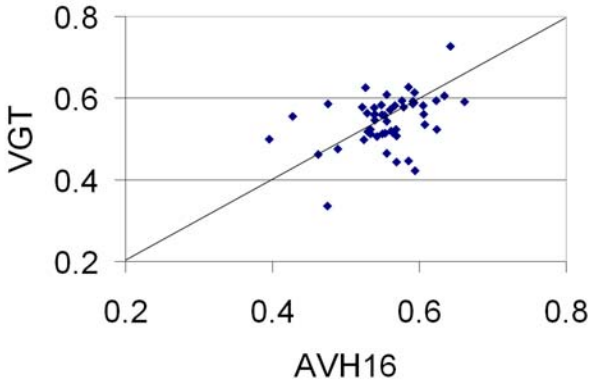

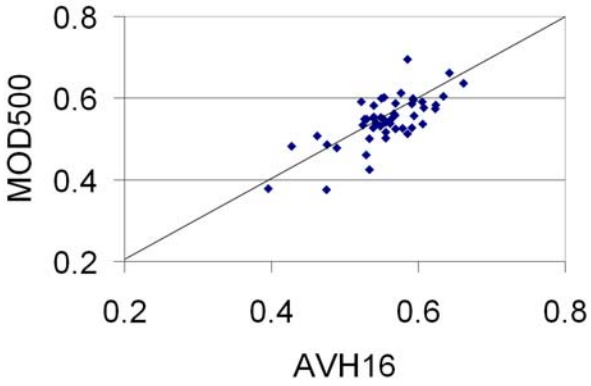

MOD500 = 37º(X=1, Y=-1), AVH16 = 45º (X=-27, Y=-18), VGT = 36º (X=68, Y=-15)

(Miura et al., 2010, in prep.)

Agreement Analysis & Coefficient (Ji & Gallo, 2006)

- The agreement coefficient (AC) considers that both *x*- and *y*-variables are subject to random errors.

- The AC measures the *systematic* ($RMPD_S$) and *unsystematic* ($RMPD_U$) components of the root mean square difference (RMSD):

$$RMSD = \sqrt{\left(RMPD_S\right)^2 + \left(RMPD_U\right)^2}$$

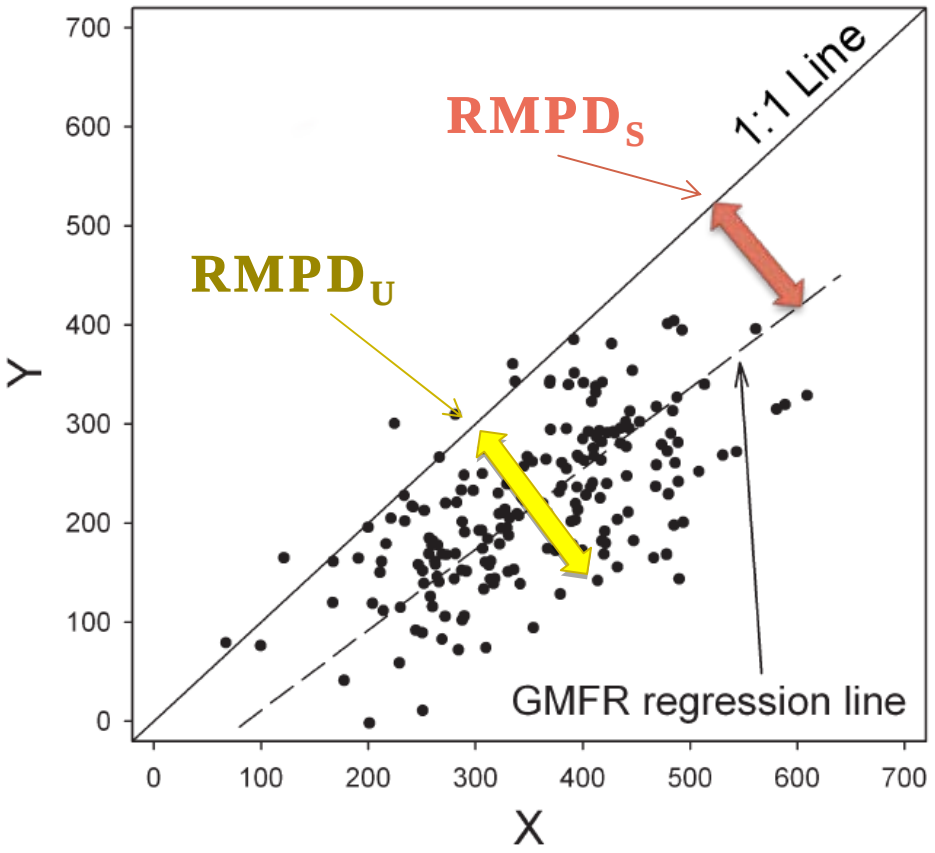

Agreement Coefficients over CONUS (1 km): MODIS, AVHRR/2, AVHRR/3, vs. VEGETATION

NDVI

Sensor (Y vs. X)	$RMPD_S$	($RMPD_U$)	GMFR	R^2
MOD vs. MYD	.007	(± .032)	Y = .004 +1.006 X	.98
MOD vs. VGT4	.035	(± .039)	Y = .048 + .971 X	.96
MOD vs. AVHRR/3	.022	(± .049)	Y = -.047 +1.111 X	.94
VGT4 vs. AVHRR/2	.038	(± .042)	Y = -.132 + 1.226 X	.95

EVI2

Sensor (Y vs. X)	$RMPD_S$	($RMPD_U$)	GMFR	R^2
MOD vs. MYD	.003	(± .026)	Y = .001 + 1.009 X	.98
MOD vs. VGT4	.031	(± .029)	Y = .004 + 1.102 X	.96
MOD vs. AVHRR/3	.032	(± .038)	Y = -.044 + 1.231 X	.94
VGT4 vs. AVHRR/2	.021	(± .047)	Y = -.047 + 1.098 X	.95

(Miura et al., 2010, in prep.)

Global Coarse Resolution (0.05º) Daily Products:
Terra MODIS vs. SPOT-4 VEGETATION

NDVI

Sensor (Y vs. X)	$RMPD_S$ ($RMPD_U$)	GMFR	R^2
***Original* (5%)**			
MOD vs. VGT4	.025 (± .045)	Y = .016 +1.034 X	.95
***Translated* (5%)**			
MOD vs. ML-VGT4	<.001 (± .043)	Y = -.001 +1.004 X	.95

EVI2

Sensor (Y vs. X)	$RMPD_S$ ($RMPD_U$)	GMFR	R^2
***Original* (5%)**			
MOD vs. VGT4	.027 (± .032)	Y = .010 +1.102 X	.91
***Translated* (5%)**			
MOD vs. ML-VGT4	.001 (± .032)	Y = -.002 +1.010 X	.91

(Tsend-Ayush et al., 2010, in prep.)

Global Coarse Resolution (0.05º) Daily Products:
Cross-calibration/Translation Results

$$NDVI_{VGT4,\ MODIS\text{-}like} - NDVI_{MODIS} < \pm .05$$

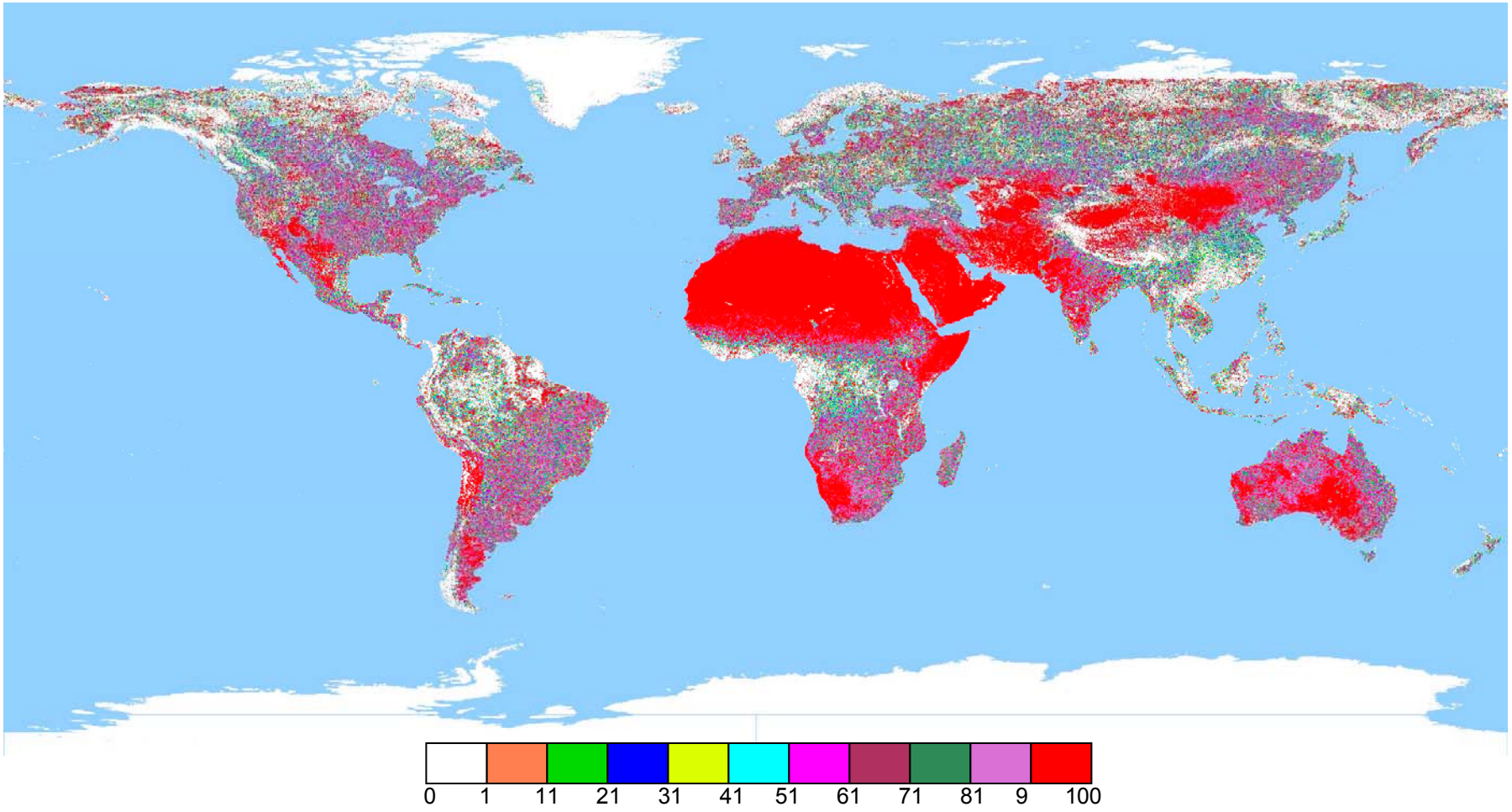

(Tsend-Ayush et al., 2010, in prep.)

Summary & Future Direction

- Bottom-up to understand and model the effects of sensor characteristics and algorithm differences for cross-calibration
- Top-down to evaluate and validate the studied effects via the bottom-up approach or cross-calibration results

- Factor-by-factor analyses
  - Hyperspectral data
- Algorithm differences in top-down evaluation
  - In-house processing
- Top-down evaluation methodologies
  - ±.05 for NDVI & EVI2
  - Uncertainty estimation method

End of Slide Show

ASTER and MODIS Instrument Characteristics

	ASTER (Yamaguchi et al., 1998)	**MODIS** (Justice et al., 2002)
Swath Width	VNIR[a] & SWIR[a]: 60 km, push-broom TIR[a]: 60 km, cross-track scanning ± 24° cross-track pointing for VNIR ± 8.55° cross-track pointing for SWIR & TIR	2,330 km, whisk-broom ± 55° cross-track scanning
Spectral Bands	14 bands, between 0.520 and 11.650 μm	36 bands, between 0.405 and 14.385 μm
Spatial Resolutions at Nadir	15 m (VNIR: bands 1-3) 30 m (SWIR: bands 4-9) 60 m (TIR: bands 10-14)	250 m (bands 1-2) 500 m (bands 3-7) 1,000 m (bands 8-36)
Radiometric Resolution	8 bits	12 bits
Geolocation Accuracy	± 50 m (1 s.d.[b] at nadir) (Iwasaki & Fujisada, 2005)	± 50 m (1 s.d. at nadir) (Wolfe et al., 2002)

[a] ASTER consists of the three subsystems: the visible/near-infrared (VNIR), shortwave-infrared (SWIR), and thermal infrared (TIR) subsystems.
[b] Standard deviation.

(Miura et al., 2008)

Sensitivities of NDVI Relationships to Atmospheric Correction Schemes

Konza Prairie, Kansas

- 6S+SAIL2
- AERONET, TOMS
- Sun/view geometry from satellites
- FIFE canopy parameters

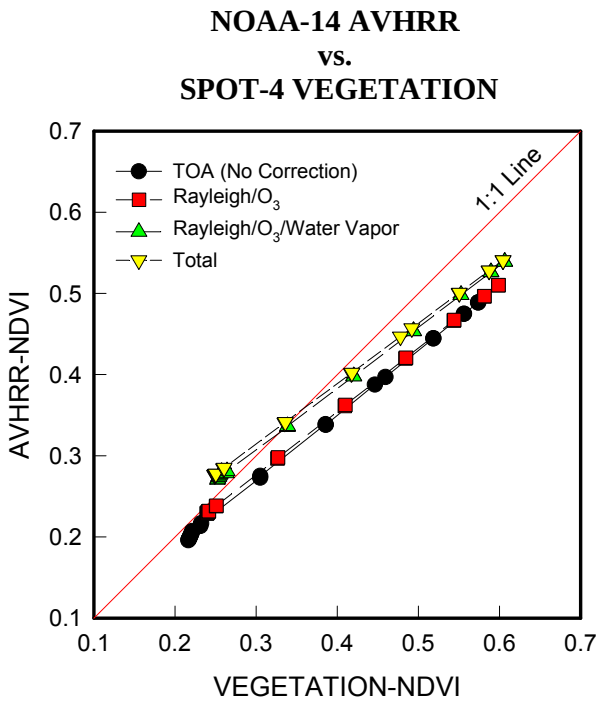

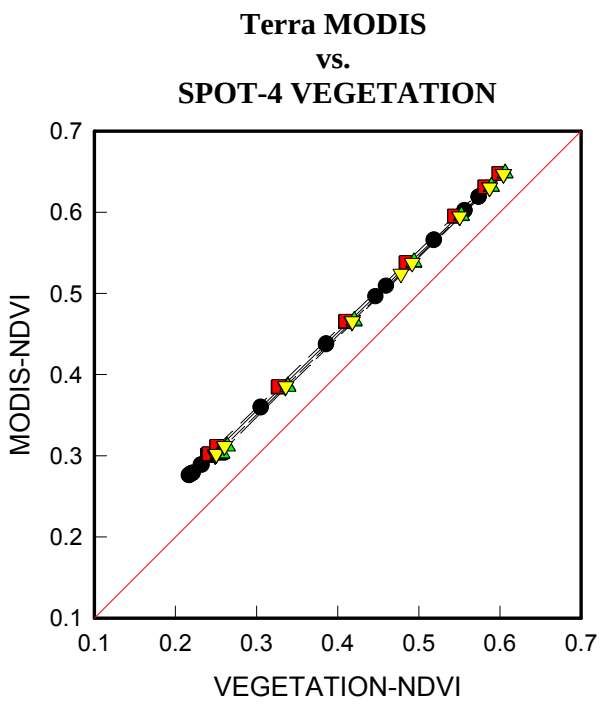

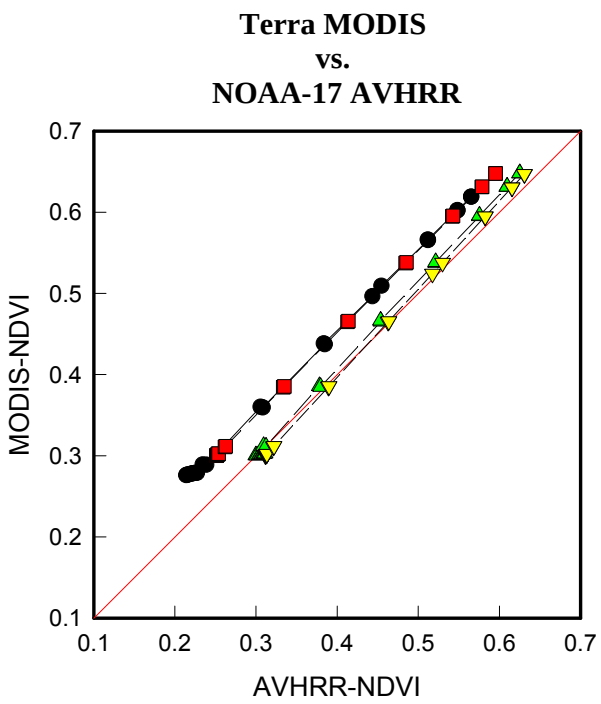

NDVI – Agreement Analysis over CONUS

Sensor (Y vs. X)	$RMPD_S$	($RMPD_U$)	GMFR	R^2
MOD vs. MYD	.007	(± .032)	Y = .004 +1.006 X	.98
MOD vs. VGT4	.035	(± .039)	Y = .048 + .971 X	.96
MOD vs. AVHRR/3	.022	(± .049)	Y = -.047 +1.111 X	.94
VGT4 vs. AVHRR/2	.038	(± .042)	Y = -.132 + .226 X	.95

EVI – Agreement Analysis over CONUS

Sensor (Y vs. X)	$RMPD_S$	($RMPD_U$)	GMFR	R^2
MOD vs. MYD	.002	(± .024)	Y = .002 + .999 X	.98
MOD vs. VGT4	.038	(± .028)	Y = -.001 +1.151 X	.96

EVI2 – Agreement Analysis over CONUS

Sensor (Y vs. X)	$RMPD_S$	($RMPD_U$)	GMFR	R^2
MOD vs. MYD	.003	(± .026)	Y = .001 + 1.009 X	.98
MOD vs. VGT4	.031	(± .029)	Y = .004 + 1.102 X	.96
MOD vs. AVHRR/3	.032	(± .038)	Y = -.044 + 1.231 X	.94
VGT4 vs. AVHRR/2	.021	(± .047)	Y = -.047 + 1.098 X	.95

AVHRR
Off Nadir vs Nadir

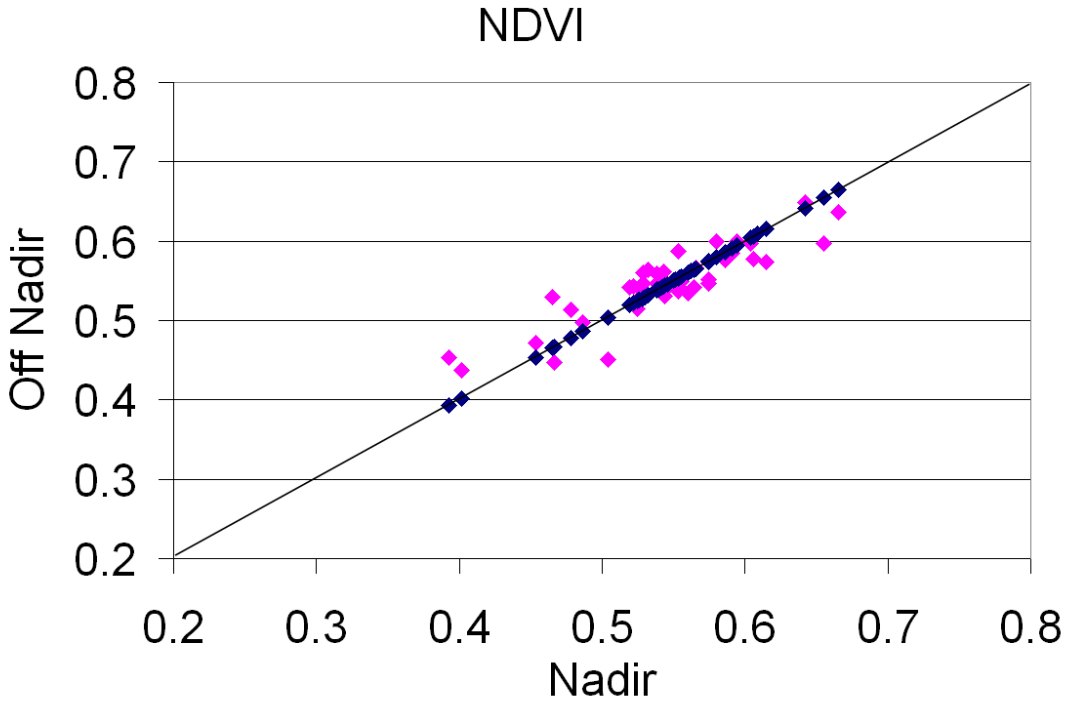

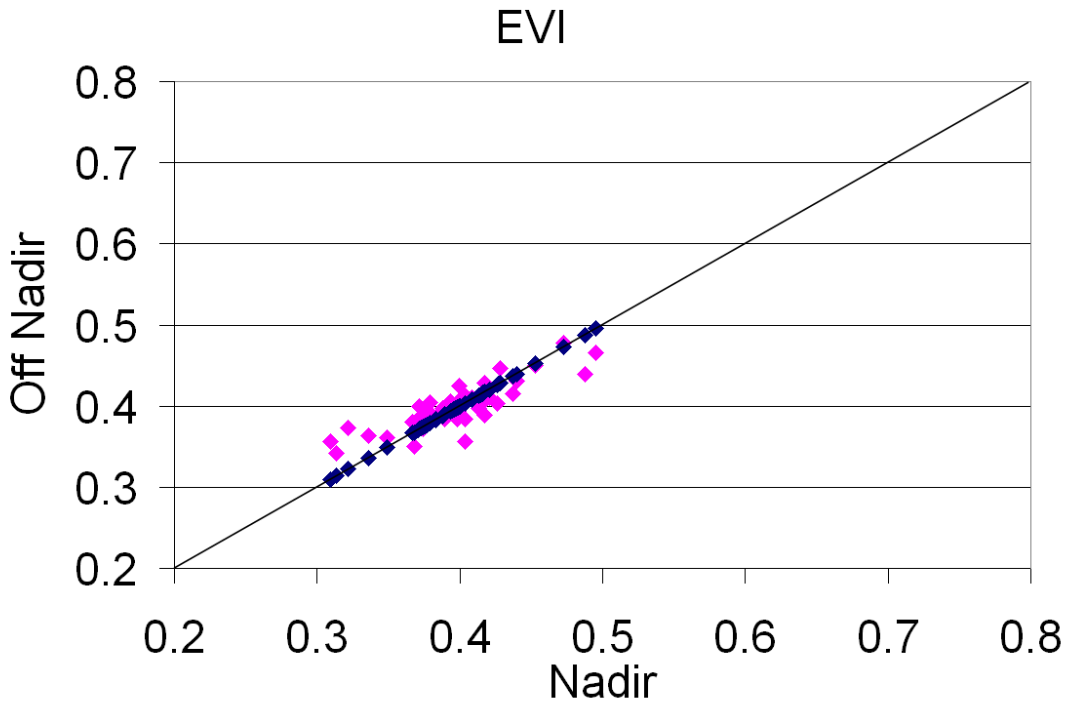

AVHRR 16
Off Nadir vs Nadir

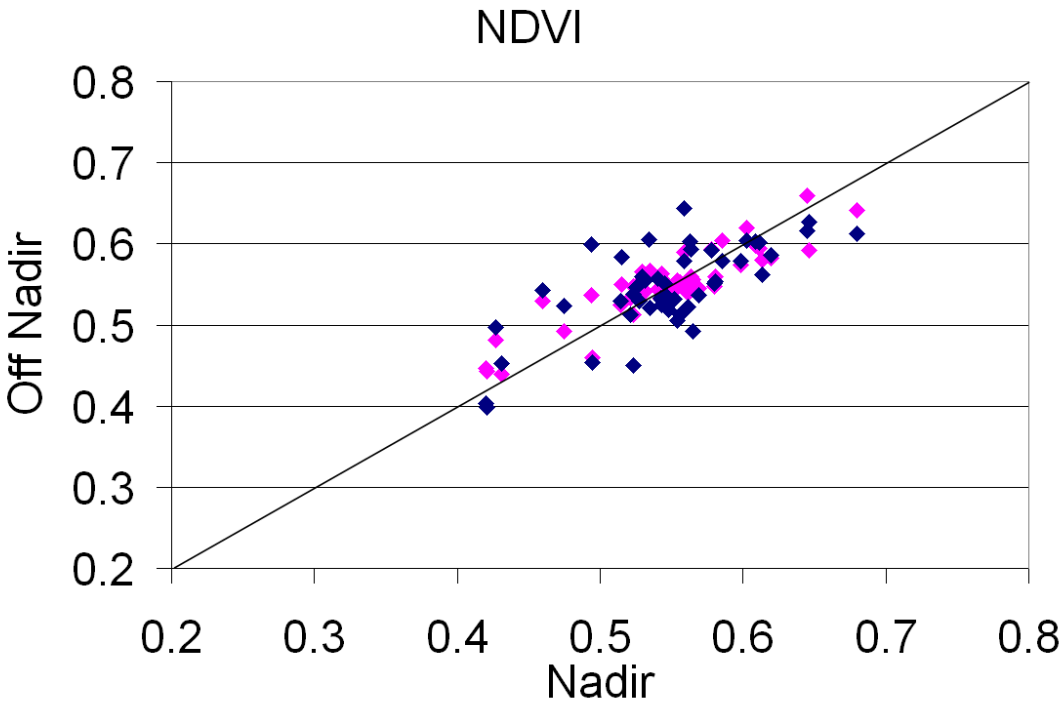

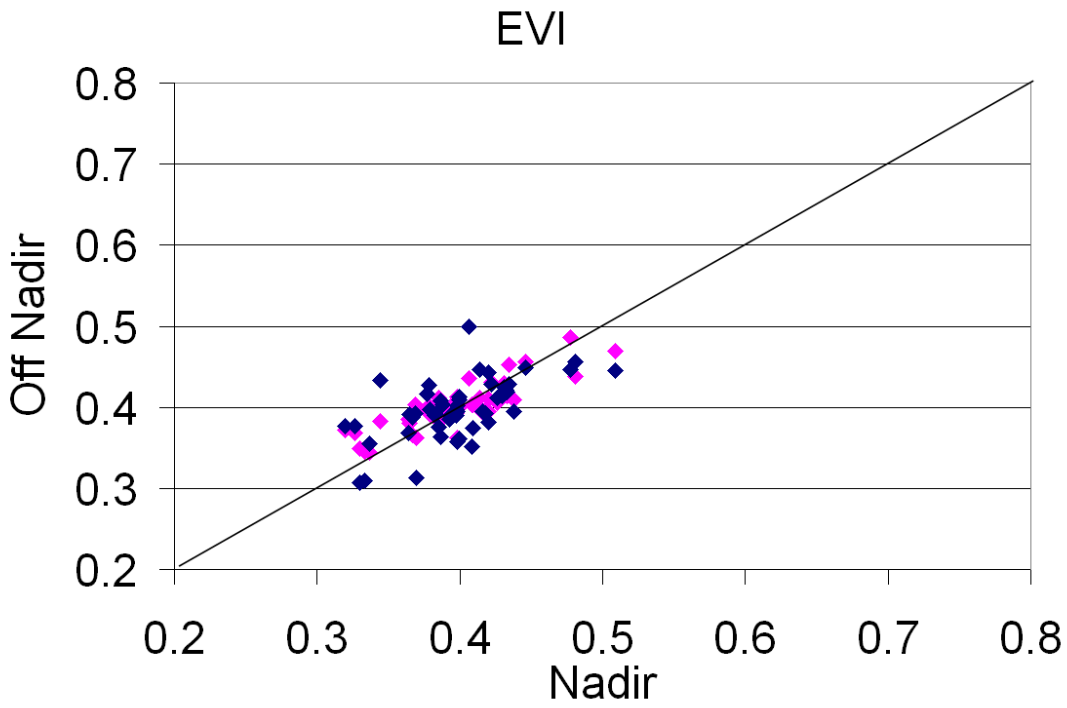

ViewZenith=55
ViewZenith=5

Geolocation Error (m)

X=-480, Y=30 (Angle=55)

X=540, Y=-900 (Angle=5)

Bottom-up: Atmosphere